

Experimental modal analysis of a beam travelled by a moving mass using Hilbert Vibration Decomposition

Mathieu BERTHA, Jean-Claude GOLINVAL

Aerospace & Mechanical Engineering Department, Faculty of Applied Sciences, University of Liège, Liège, Belgium
 email: mathieu.bertha@ulg.ac.be, jc.golINVAL@ulg.ac.be

ABSTRACT: In this paper the problem of modal identification of time-varying system is investigated. To do so, a technique based on the sifting process of the Hilbert Vibration Decomposition (HVD) method is presented. The key idea is to estimate the instantaneous frequency of the dominant mode, to extract its corresponding component by demodulation of the recorded signals and then to iterate with the subsequent dominant mode. In the case of multiple recorded signals, a source separation method is used as a preprocessing step to facilitate the identification of the instantaneous frequency for the following demodulation step. To illustrate the method, an experimental set-up consisting in a beam travelled by a non negligible mass is considered. The whole structure is randomly excited during the travel of the mass and some responses on the beam are recorded.

KEY WORDS: Modal identification; Time-varying systems; Hilbert transform; Instantaneous frequency.

1 INTRODUCTION

Recently the field of identification of time-varying systems has known a great increase of interest.

As the dynamic response of time-varying systems is non-stationary, identification of such systems requires appropriate signal processing tools. One of the most known technique is the *Empirical Mode Decomposition (EMD)* method [1] which is able to split a signal into its mono-components.

More recently, the *Hilbert Vibration Decomposition (HVD)* method [2] was introduced with the same goal of splitting signals into their constitutive mono-components. The present work is based on this technique.

The paper is organized as follows. First, the definition of the Hilbert Transform and both the EMD and HVD methods are briefly recalled in Sections 2, 3 and 4. Additional signal processing tools are introduced in the HVD method to extend its application to multiple degrees-of-freedom (MDOF) systems. The proposed method is then applied to the identification of a time-variant system. The system studied in this work is a beam on which a mass, which is not negligible with respect to the mass of the beam, is moving. This system is presented in Section 6 together with the results of the modal identification of the beam subsystem only (*Linear Time Invariant (LTI)* system) which are used as reference modal properties. Finally a conclusion ends the paper.

2 THE HILBERT TRANSFORM

For seek of clarity, the definition of the Hilbert transform along with some of its properties which will be used later in the EMD and HVD methods are briefly recalled.

The Hilbert transform is a particular transform that remains in the same domain as the processed signal (the time domain in our case). It is defined as the convolution product between the signal and the function $h(t) = \frac{1}{\pi t}$:

$$\mathcal{H}(x(t)) = \frac{1}{\pi} \text{p.v.} \int_{-\infty}^{+\infty} \frac{x(\tau)}{t - \tau} d\tau \quad (1)$$

in which p.v. stands for the Cauchy principal value of the integral in (1). It results in a signal which is phase shifted by $-\frac{\pi}{2}$ radian. Thus the analytic form of the initial signal is built by adding the imaginary unit times the Hilbert transform of itself, i.e.

$$\begin{aligned} z(t) &= x(t) + i\mathcal{H}(x(t)) \\ &= a(t)e^{i\phi(t)}, \end{aligned} \quad (2)$$

where $a(t)$ and $\phi(t)$ are instantaneous amplitude and phase of the signal, respectively. The instantaneous frequency can then be calculated by taking the time derivative of the instantaneous phase, $\omega_k(t) = \dot{\phi}_k(t)$, but it is important to note that it is meaningful only if applied on mono-components. Indeed, for instance in the case of a multi-components signal, the instantaneous frequency calculated in such a way can be occasionally negative.

The Hilbert Vibration Decomposition method described in section 4 will make use of the analytic form of the signal to perform separation into mono-components.

2.1 Properties of the Hilbert transform

To apply the Hilbert transform to modal analysis, let us recall two properties of the Hilbert transform:

Derivative: The Hilbert transform of the (k^{th} -)derivative of a signal is the (k^{th} -)derivative of the Hilbert transform of this signal:

$$\mathcal{H}\left(\frac{d^k x(t)}{dt^k}\right) = \frac{d^k}{dt^k}\left(\mathcal{H}(x(t))\right). \quad (3)$$

The Bedrosian's theorem [3]: If a signal is itself the product of two signals, one slowly varying and the second fast varying, the Hilbert transform of this product is equal to the slowly varying signal times the Hilbert transform of the fast one under a particular condition. The latter condition implies that, if one computes the spectrum of the slow and fast signals, they must not overlap. In that case, if $f(t)$ and $g(t)$ are the slow and fast signals, respectively and if the non-overlapping condition is fulfilled, one has:

$$\mathcal{H}(f(t)g(t)) = f(t)\mathcal{H}(g(t)). \quad (4)$$

Let us consider the equation of motion of a multiple degrees-of-freedom (MDOF) time-variant dynamical system:

$$\mathbf{M}(t)\ddot{\mathbf{x}}(t) + \mathbf{C}(t)\dot{\mathbf{x}}(t) + \mathbf{K}(t)\mathbf{x}(t) = \mathbf{f}(t). \quad (5)$$

Now let us add to equation (5) its Hilbert transform multiplied by the complex unit. According to the properties (3) and (4), the analytic form of the motion equation (5) writes:

$$\begin{aligned} & \mathbf{M}(t)\ddot{\mathbf{x}}(t) + \mathbf{C}(t)\dot{\mathbf{x}}(t) + \mathbf{K}(t)\mathbf{x}(t) = \mathbf{f}(t) \\ & + i \times \mathcal{H}\left(\mathbf{M}(t)\ddot{\mathbf{x}}(t) + \mathbf{C}(t)\dot{\mathbf{x}}(t) + \mathbf{K}(t)\mathbf{x}(t)\right) = \mathcal{H}\left(\mathbf{f}(t)\right) \end{aligned}$$

$$\mathbf{M}(t)\dot{\mathbf{z}}(t) + \mathbf{C}(t)\dot{\mathbf{z}}(t) + \mathbf{K}(t)\mathbf{z}(t) = \mathbf{g}(t) \quad (6)$$

3 EMPIRICAL MODE DECOMPOSITION AND THE HILBERT-HUANG TRANSFORM

The aim of the EMD method is to sift a signal into constitutive mono-components which are named *Intrinsic Mode Functions (IMFs)*. To this purpose, the signal $x(t)$ is assumed to be modelled as

$$x(t) = \sum_k a_k(t) \cos(\phi_k(t)) + n(t), \quad (7)$$

where $a_k(t)$ and $\phi_k(t)$ are instantaneous amplitude and phase of the k^{th} mono-component, respectively. $n(t)$ is added to model the noise present in the signal.

In this method, the sifting process is based on cubic-spline interpolation of all the maxima and all the minima in the signal which lead to the upper and lower envelopes of the signal. The mean of these two envelopes is then calculated and retrieved from the signal. This process is iterated until the resultant signal has a local mean equal to zero and until the number of extrema and zero crossing does not differ of more than one. The two latter conditions correspond to the definition of an IMF. Once they are fulfilled, the IMF can be extracted from the initial signal and the whole process is repeated for the extraction of the next IMFs.

Once all the IMFs are extracted from the signal, it remains to compute their instantaneous properties. This is done using of the *Hilbert transform* (described in Section 2) and the analytic form of the signal in addition to the EMD method. This combination is called the *Hilbert-Huang transform (HHT)* [1].

4 THE HILBERT VIBRATION DECOMPOSITION METHOD

The Hilbert Vibration Decomposition method [2] uses the analytic form of a signal to extract its mono-components from the highest to the lowest instantaneous amplitude. In the following, one will refer to the *dominant mode* for the component having the highest instantaneous amplitude.

The HVD method is based on the following analytic representation of the multi-components signal in the complex domain:

$$\begin{aligned} z(t) &= a(t)e^{i\phi(t)} \\ &= \sum_k a_k(t)e^{i\phi_k(t)}. \end{aligned} \quad (8)$$

This multi-components model in the complex domain can be seen as a sum of rotating phasors corresponding to each component, each one having its own amplitude $a_k(t)$ and phase $\phi_k(t)$. So, the trajectory in the complex plane is driven by the dominant mode (highest a_k) around which the other components add some oscillations. This is illustrated in Figure 1 in the particular case of a two-components signal with constant amplitudes and frequencies. The way to recover the dominant

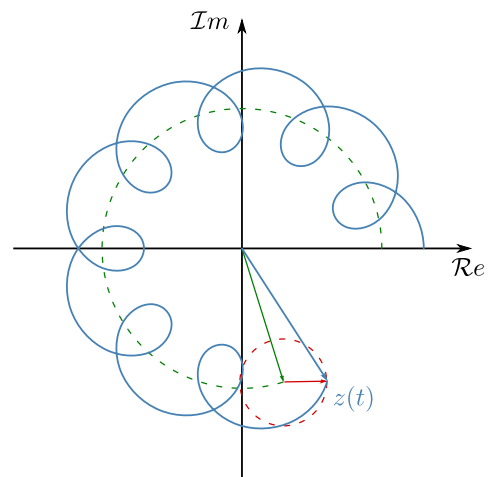


Figure 1. Trajectory in the complex plane of a two-components signal with constant amplitudes and frequencies. The second component causes the signal to oscillate around the trajectory of the dominant component

component by the HVD method is to low-pass the phase of the signal to filter the oscillations due to the secondary component(s) and isolate the phase evolution of the dominant mode. The latter is used for the extraction of the dominant component by synchronous demodulation. Once the dominant component is extracted from the signal, the process is repeated for the extraction of new dominant components.

5 EXTENSION OF THE HVD METHOD TO MDOF SYSTEMS

5.1 Limitations of the EMD and HVD methods

To be used for modal identification purpose, the mono-components provided by both the HVD and EMD methods should ideally correspond to one particular (time-varying) mode of vibration, but to this end both methods have a weak point. Indeed, each method extracts the component having the highest instantaneous frequency (in the EMD method) or amplitude (in the HVD method). It follows that, if in the multi-components mixture there are crossings in frequency or amplitude between mono-components, both methods will follow these crossings. It will result that the extracted components may contain jumps between different vibration modes.

5.2 Improvement of the HVD method

To overcome possible jump phenomena mentioned in the previous subsection, add-in are proposed to the algorithm presented in [2] in order to handle MDOF systems. The main modification of the algorithm is the addition of a source separation method. Indeed, using a source separation technique on multiple channels helps to make a preparatory separation of the modes. Then using a separated source as input to the decomposition algorithm reduces the occurrence of mode switching. Further, to apply the initial algorithm on a MDOF system, one has to do it in parallel on each channel. Doing this in that way results in one frequency curve (and the corresponding demodulated component) per channel. In that case, the mode switching phenomenon can easily occur and nothing ensures that switches will occur at the same time. So, using one separated source in the algorithm gives one frequency curve that is used to demodulate its corresponding component on all the channels simultaneously. The source separation technique used in the present work is the *Second-Order Blind Identification (SOBI)* method [4].

A second improvement in the initial algorithm is to replace the synchronous demodulation step. In the initial algorithm the instantaneous frequency was obtained by low-pass filtering of the instantaneous frequency and then used for the synchronous demodulation. In our case, the phase is first smoothed by a trend detection technique (a Hodrick-Prescott filter [5] here) and then used in a Vold-Kalman filter [6] for the extraction of its corresponding component. It has the advantage to be able to simultaneously demodulate multiple components even in the presence of frequency crossings.

In short, the Hodrick-Prescott filter models a signal as a trend $\tau(t)$, oscillatory components $c(t)$ and noise $n(t)$:

$$\phi(t) = \tau(t) + c(t) + n(t) \quad (9)$$

Applied to the phase of the analytic signal, the goal is to extract the trend of the phase, which corresponds to the phase of the dominant mode. In the Hodrick-Prescott method, the trend,

$\tau(t)$, is found by solving an optimisation problem :

$$\min_{\tau} \left[\sum_{t=1}^T (\phi_t - \tau_t)^2 + \lambda \sum_{t=2}^{T-1} ((\tau_{t+1} - \tau_t) - (\tau_t - \tau_{t-1}))^2 \right]. \quad (10)$$

The first term penalizes strong deviations from the trend and the second penalizes fast variations of the trend. λ is a smoothing parameter which tunes the smoothness of the trend.

The signal model in the Vold-Kalman filter is the same as in (8). The Vold-Kalman filter is able to recover the complex amplitude $a_k(t)$ when the signal and the instantaneous phase $\phi_k(t)$ are provided. It is composed of two equations, the data equation:

$$x(t) - \sum_k a_k(t) e^{i\phi_k(t)} = \delta(t) \quad (11)$$

and the structural equation:

$$\nabla a_k(t) = \varepsilon_k(t), \quad (12)$$

in which $\delta(t)$ and $\varepsilon_k(t)$ have to be minimized to get the complex envelopes $a_k(t)$ in the signal. In Equation (12), ∇ represents a difference operator and, as in the Hodrick-Prescott filter, this equation adds a smoothness constraint on the result.

Applying the Vold-Kalman filter leads to express the signal as a series of complex envelopes multiplied by a time oscillation function at an instantaneous eigen-frequency of the system. The similarity with the modal expansion of linear systems is evident and the complex envelopes obtained in that way may be assimilated to instantaneous unscaled mode-shapes:

$$\begin{aligned} \text{Vold-Kalman filter: } x(t) &= \sum_k \mathbf{a}_k(t) e^{i\phi_k(t)} \\ &\quad \updownarrow \quad \updownarrow \\ \text{Modal expansion: } x(t) &= \sum_k \mathbf{V}_k(t) \eta_k(t) \end{aligned} \quad (13)$$

Finally, the k^{th} component of the signal is obtained by taking the real value of the multiplication between the complex envelope and its corresponding phasor:

$$x_k(t) = \mathcal{R}e \left(a_k(t) e^{i\phi_k(t)} \right) \quad (14)$$

Once $x_k(t)$ is obtained, it is removed from the signal and the next component can be extracted. The full algorithm is summarized in the flow chart of Figure 2.

6 EXPERIMENTAL SET-UP AND TIME-VARIANT ANALYSIS

6.1 Set-up description

The example of application considered in this study consists in a beam loaded by a travelling mass, what confers to the system its time-variant behaviour.

The beam is a 2.1 m long aluminium beam with a rectangular cross section of 8×2 cm. As boundary conditions, each end of the beam is connected to a steel box through roller bearings in order to enable free rotations at both ends. Finally, these boxes

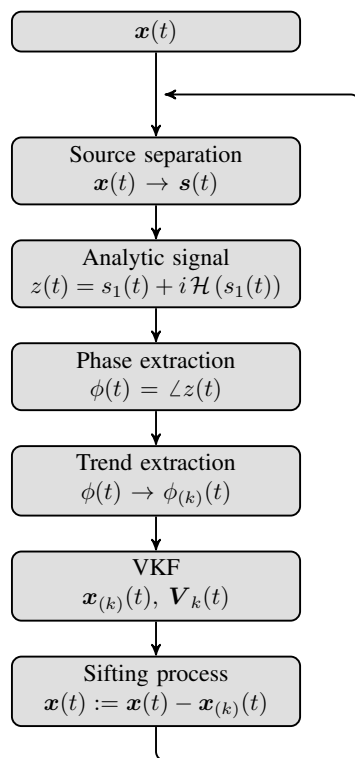


Figure 2. Flow chart of the method.

are fixed on springs to elevate the structure and to facilitate the placement of the shaker and accelerometers under the beam.

The moving mass consists in a 3.475 kg steel block. With respect to the mass of the beam (9 kg), it corresponds to a ratio of 38.6 %.

The excitation set-up consists in one shaker applying a random force on the structure. Seven accelerometers are placed along the neutral axis of the beam to measure the bending modes. Their locations are $x = \{0, 0.4, 0.7, 1.05, 1.4, 1.7, 2.1\}$ m, respectively, the reference frame being located at the left hand side of the beam (as shown in Figure 3). Data acquisition and signal processing are performed using the LMS SCADAS Mobile and the LMS Test.Lab software [7, 8] respectively.

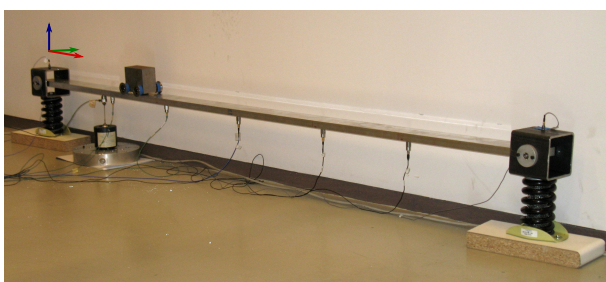


Figure 3. Setup description.

6.2 Modal testing of the unloaded beam (LTI system)

A standard modal testing is first performed on the unloaded beam. To this end, the structure is excited by a random force and

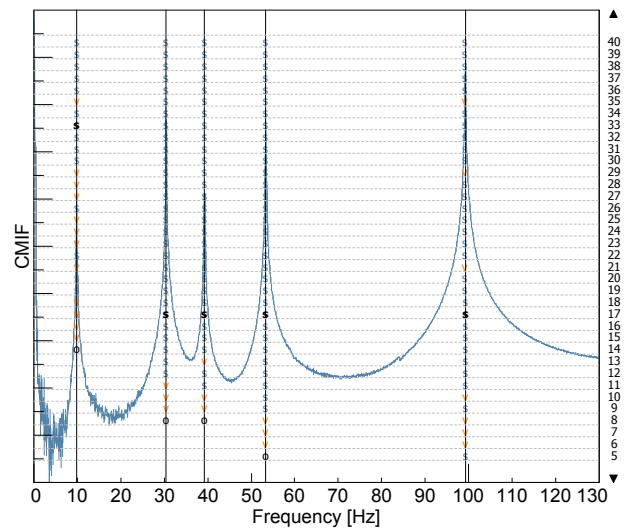


Figure 4. Stabilisation diagram of the unloaded beam (LTI system). Tolerances: 1% vector, 1% frequency, 1% damping.

the dynamic response is recorded by the seven accelerometers. Modal identification is performed using the PolyMAX method [9] implemented in the LMS Test.Lab environment. The resulting stabilisation diagram and the selected modes are shown in Figure 4 and are listed in Table 1.

Table 1. Experimental eigen-frequencies and damping ratio's of the unloaded beam

Mode #	Frequency f_r [Hz]	Damping ratio ζ_r [%]
1	9.80	0.22
2	30.43	0.10
3	39.23	0.20
4	53.32	0.08
5	99.22	0.07

The mode-shapes corresponding to the five first modes are plotted in Figure 5.

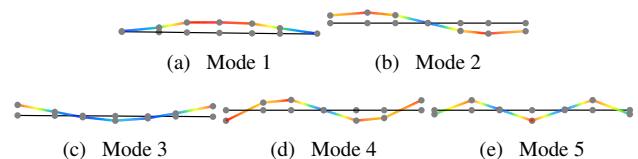


Figure 5. Experimental mode shapes of the beam subsystem.

6.3 Identification of the time-varying system

In this section, the dynamics of the beam loaded by the travelling mass is examined. To this end, the mass is slowly pulled along the beam while the beam is excited by a random force. To have a first idea of the time-varying dynamics of the system, the wavelet spectra of the second sensor (at 0.4 m) is given in Figure 6.

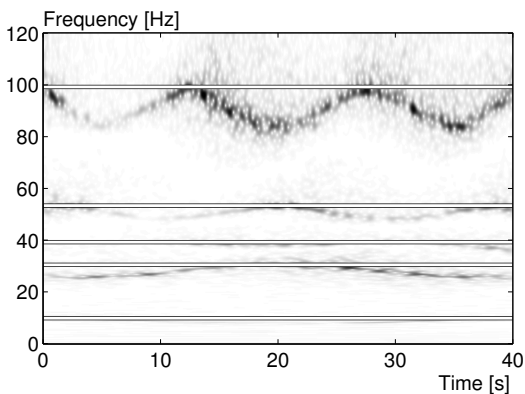


Figure 6. Wavelet spectra of the response of the second sensor. The frequencies of the beam subsystem only are shown as white dashed lines.

In Figure 6, several properties can be observed. First, it appears that the first mode (close to 10 Hz) is not significantly excited in the response. This is also the case in the other channels. Second, the frequency variation due to the motion of the mass is clearly visible. It appears as variations with top values very close to the frequencies of the unloaded beam. In the measurement process, the mass was pulled at an approximately constant speed so that the time axis can be broadly linked to the longitudinal axis of the beam. For each mode in Figure 6 the frequency oscillates between minimum and maximum values and if we compare with the mode-shapes shown in Figure 5, we can easily see that the times when the frequency comes back to the frequency of the unloaded beam correspond to the time instants when the mass is located to a node of vibration of the structure. In that configuration, the mass does not participate to the mode so that the system has the same properties as the initial one. On the contrary, when the mass is located at an anti-node of vibration, its participation to the system inertia is maximum so that the frequency decay is maximum. The last thing that can be observed is that higher the frequency is, more important is the perturbation due to the mass.

6.4 Application of the proposed identification algorithm

The HVD method is applied here with the modifications proposed in Section 5.2.

6.4.1 Extraction of instantaneous frequencies and components

The first step is to apply the source separation technique (the SOBI method is considered here) on all the channels. In Figure 7, the first computed source is illustrated. It broadly corresponds to the vibration frequency of the fifth mode. Next, the instantaneous unwrapped phase of this source is calculated by the use of its Hilbert transform and the analytic form of the source. The unwrapping avoids the 2π radians jumps in the phase calculation. The phase is then smoothed using the Hodrick-Prescott filter to remove the perturbations due to the

residue of the other modes and the instantaneous frequency is calculated by time derivation. The instantaneous frequency corresponding to that mode is shown by the white dashed line in Figure 7.

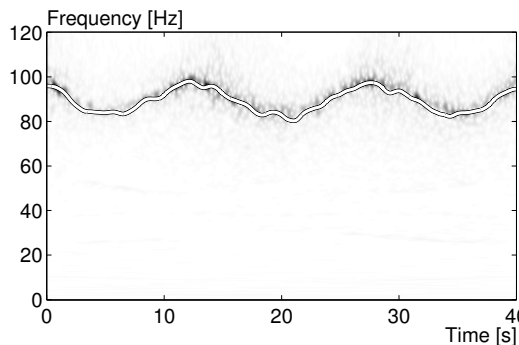


Figure 7. Wavelet spectra of the first source computed by the SOBI method. The instantaneous frequency calculated by the use of the Hilbert transform is shown as a white dashed line.

Once the instantaneous phase is known, it can be used to extract the corresponding component in each channel using the Vold-Kalman filter and equation (14).

For instance, the resulting component of the fifth mode and the modulus of its amplitude are shown in Figure 8.

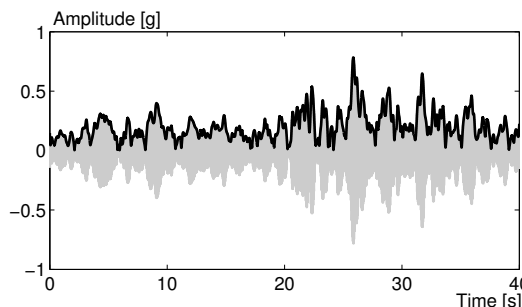


Figure 8. The extracted component corresponding to the fifth mode (gray) in the second channel and its amplitude (black) with respect to time.

Once computed on each channel, the mono-components are subtracted from their corresponding signal and the algorithm is repeated for the extraction of the next mode.

After four iteration steps, the modes from two to five are extracted from the response of all accelerometers. The first mode is not enough excited to be well extracted by the method. The identified instantaneous frequencies of the system are shown in Figure 9 with the wavelet spectra of the channel 2 as background support.

6.4.2 Correlation of instantaneous modal deformations

As described in Section 5.2, the Vold-Kalman filter is able to calculate the complex amplitude corresponding to a phase

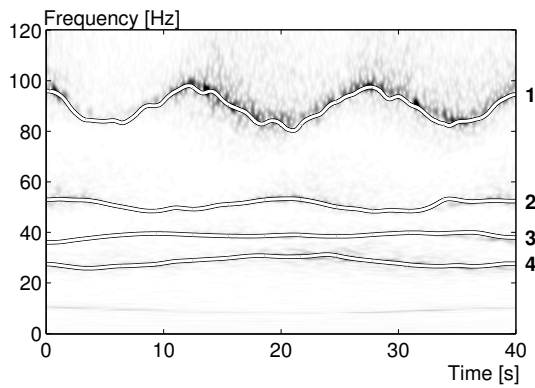


Figure 9. Instantaneous frequencies identified by the method after four iterations. Numbers on the right vertical axis indicates the order of extraction.

signal. With equation (13), we have seen that the complex amplitudes can be seen as unscaled mode-shapes.

In the case of linear time-variant systems, the natural frequency and mode-shape associated to a specific complex amplitude and phase signal vary with time. To have an idea of the correlation between the reference mode-shapes (those calculated on the LTI unloaded beam) and the identified time-variant mode-shapes (taking into account the moving mass), the MAC criteria is used instantaneously. It means that, at each time instant, the MAC matrix is calculated between the reference modes and the instantaneous mode-shapes. Because of the additional time variable, the MAC layout has to be modified for graphical representation. To do so, at each time instant, the calculated MAC matrix is reshaped in a column vector. Then all the MAC vectors corresponding to one time instant are concatenated in a global TV-MAC matrix as illustrated in Figure 10. Whereas in LTI modal analysis a unitary diagonal corresponds to perfect matching, here a perfect matching will be given by unitary rows facing the right couples of similar modes.

On that time-varying MAC matrix, some characteristics of the system can be seen. First, the global shape of the matrix shows that the time-varying mode-shapes remain more or less well correlated to the reference mode-shapes. Second, looking to one specific correlated row, some drops of correlation appear periodically, especially on the highest frequency modes. These drops are due to mode-shape distortions caused by the presence of the moving mass. This is exactly the same phenomenon as explained in Section 6.3 where the instantaneous frequencies show their maximum decrease when the mass passes at anti-nodes of vibration. Concerning the mode-shapes, it is also in those configurations that the effect of the mass is the most significant.

As an example, let us take the fourth time-varying identified mode-shape which correlates with the fifth mode-shape of the unloaded beam and let us consider the particular time instants $t = \{6, 12, 20, 28, 34\} s$. The evolution of the fourth mode-shape at these time instants is illustrated in Figure 11.

First it can be seen that the instantaneous mode-shapes taken

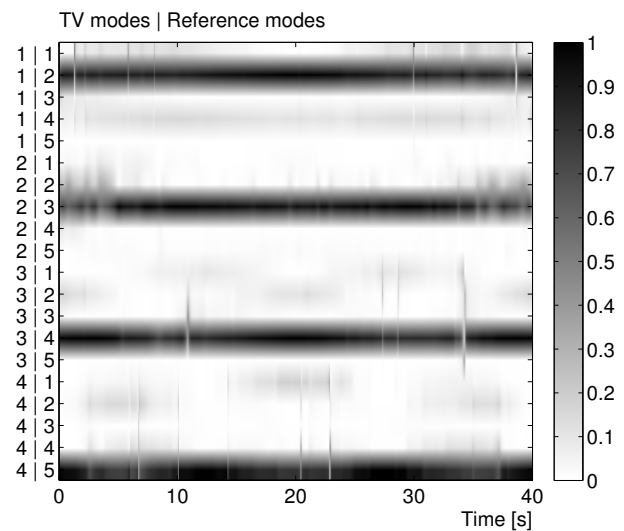


Figure 10. Time-varying modal assurance criterion. The y-axis label indicates the couple of modes which are compared and the time dependency appears along the x-axis.

at $t = 12 s$ (Figure 11(b)) and $28 s$ (Figure 11(d)) are similar to mode 5 of the unloaded beam (LTI analysis). The corresponding frequencies of these two snapshots are 97.97 and 97.15 Hz to be compared with 99.22 Hz in the LTI analysis. The slight difference in frequency when the mass is located at these nodal positions may be due to the inertia properties of the moving mass.

Now let us take a look on Figures 11(a), 11(c) and 11(e). These three configurations correspond approximately to configurations where the moving mass is located successively at each anti-node of vibration of the fifth LTI mode-shape. It is at these positions that the added inertia force has the maximal effect on the mode-shape, decreasing the amplitude of the anti-node where it is located with respect to the other anti-nodes. At these three time instants, the identified instantaneous frequencies are 83.96, 82.88 and 82.74 Hz, respectively.

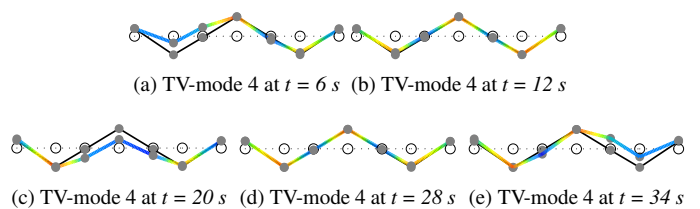


Figure 11. Fourth identified time varying mode-shape at particular times when the mass is located at nodes or anti-nodes of vibration. The undeformed beam and mode 5 from the LTI PolyMAX identification are plotted in dotted and solid lines, respectively.

7 CONCLUSION

In this work, the Hilbert Vibration Decomposition was used to perform the modal identification of a time-varying system. The addition of a source decomposition method enable the treatment

of multiple channels and decreases the risk of mode switching present in EMD and initial HVD methods.

We were able to identify the modifications on the system cause by the mass moving on the beam and its impacts on the frequencies and mode shapes of the system.

REFERENCES

- [1] N. E. Huang, Z. Shen, S. R. Long, M. C. Wu, H. H. Shih, Q. Zheng, N.-C. Yen, C. C. Tung, and H. H. Liu. The empirical mode decomposition and the Hilbert spectrum for nonlinear and non-stationary time series analysis. *Proceedings of the Royal Society A: Mathematical, Physical and Engineering Sciences*, 454(1971):903–995, 1998.
- [2] M. Feldman. *Hilbert Transform Applications in Mechanical Vibration*. John Wiley & Sons, Ltd, Chichester, UK, 2011.
- [3] E. Bedrosian. A product theorem for hilbert transforms. *Proceedings of the IEEE*, 51(5):868 – 869, 1963.
- [4] F. Poncelet, G. Kerschen, J.-C. Golinval, and D. Verhelst. Output-only modal analysis using blind source separation techniques. *Mechanical Systems and Signal Processing*, 21(6):2335–2358, 2007.
- [5] T. Alexandrov, S. Bianconcini, E. B. Dagum, P. Maass, and T. McElroy. A review of some modern approaches to the problem of trend extraction, 2008.
- [6] C. Feldbauer and R. Höldrich. Realization of a Vold-Kalman Tracking Filter - A Least Squares Problem. In *Proceedings of the COST G-6 Conference on Digital Audio Effects (DAFX-00)*, number 8, pages 8–11, Verona, Italy, 2000.
- [7] LMS SCADAS Mobile. <http://www.lmsintl.com/scadas-mobile>.
- [8] LMS Test.Lab. <http://www.lmsintl.com/testlab>.
- [9] B. Peeters, G. Lowet, V. der Auweraer, and J. Leuridan. A new procedure for modal parameter estimation. *Sound and Vibration*, (January):24–28, 2004.

